NASA Technical Memorandum 78530

High Angle of Incidence Implications Upon Air Intake Design and Location for Supersonic Cruise Aircraft and Highly Maneuverable Transonic Aircraft

Leroy S. Presley, Ames Research Center, Moffett Field, California 94035

NASA
National Aeronautics and
Space Administration

Ames Research Center
Moffett Field, California 94035

HIGH ANGLE OF INCIDENCE IMPLICATIONS UPON AIR INTAKE DESIGN AND LOCATION FOR SUPERSONIC CRUISE AIRCRAFT AND HIGHLY MANEUVERABLE TRANSONIC AIRCRAFT

Leroy L. Presley
Ames Research Center, Moffett Field, California 94035, U.S.A.

SUMMARY

Computational results which show the effects of angle of attack on supersonic mixed-compression inlet performance at four different locations about a hypothetical forebody have been obtained. These results demonstrate the power of the computational method to predict optimum inlet location, orientation, and centerbody control schedule for design and off-design performance.

The effects of inlet location and a forward canard on the angle-of-attack performance of a normal shock inlet at transonic speeds have been studied. The data show that proper integration of inlet location and a forward canard can enhance the angle-of-attack performance of a normal shock inlet.

Two lower lip treatments for improving the angle-of-attack performance of rectangular inlets at transonic speeds are discussed.

NOMENCLATURE

k $\frac{\gamma - 1}{2\gamma}$

M Mach number

n plane of known solution

p pressure

q total velocity

r radius

u Z component of velocity

v r component of velocity

w ϕ component of velocity

x horizontal coordinate

y vertical coordinate

Z longitudinal coordinate

$\bar{Z}$ longitudinal coordinate normalized by r_c

$\Delta\bar{Z}$ centerbody translation (positive forward)

δ *canard deflection angle*

α angle of attack

γ ratio of specific heats

ξ nondimensional coordinate-normalized by distance between inner and outer computational boundaries

ρ density

ϕ azimuthal coordinate

ψ angle between total velocity vector and normal to cowl-lip plane

Subscripts:

C cowl

f forebody

i indices for ξ spacing of points

j indices for ϕ spacing of points

T centerbody tip

t stagnation conditions

∞ *free-stream conditions*

1. INTRODUCTION

For most aircraft the propulsion system must be designed to maximize the net thrust when installed on the vehicle. This often requires that a compromise between drag, pressure recovery, and mass-flow capturing capability be made for the desired flight envelope of the aircraft. Changes in aircraft attitude and speed, as well as many other factors, must be considered for complete design of the propulsion system. This paper will address only the question of changes in angle of attack on inlet location and design. Two completely different types of aircraft will be considered: a supersonic cruise aircraft and a highly maneuverable, transonic aircraft.

Supersonic cruise aircraft are, for the most part, not designed to accommodate large excursions in angle of attack while at cruise conditions. The propulsion system is optimized for particular design conditions with some small margin allowed for excursions in airplane attitude. More often than not, the inlet is placed in a location to minimize upstream flow-field perturbations due to changes in airplane attitude. Precise location of the inlet is usually determined by empirical design rules or wind tunnel testing. However, recent developments in computational methods (see Refs. 1, 2) are, for the first time, providing the designer with the capability of determining the effects of angle of attack on inlet location and orientation and of determining the performance of a limited class of inlets (axisymmetric mixed-compression inlets) in three-dimensional flow fields. To demonstrate this capability, numerical solutions have been obtained for an ellipsoidal body at $M = 2.65$ and at several angles of attack. Inlet solutions are then obtained at four different flow-field locations and compared with uniform flow-field solutions. The results show computational predictions of the effects of angle of attack on inlet location for this idealized geometry. This particular configuration demonstrates both the effects of fuselage shielding and the highly nonuniform flow around the sides of the aircraft.

Highly maneuverable, transonic aircraft, on the other hand, are required to accommodate large excursions in airplane attitude. Inlets for such aircraft are required to either operate satisfactorily over a larger change in aircraft attitude, or to be located such that aircraft components successfully shield the inlet from incidence changes due to excursions in aircraft attitude. At the same time, these inlets must not detract from the net thrust production of the propulsion system over the complete flight envelope of the aircraft. For aircraft that are required to have some supersonic capability, the latter requirement usually dictates that the inlets have rather sharp lips, which in turn are deleterious to their performance at high angles of attack.

Although some progress, which will be discussed, is being made, adequate computational codes for solving complex three-dimensional flows at transonic speeds are not available. Designers for the most part, must rely on empirical data from previous wind-tunnel tests or conduct new, and often very costly, wind-tunnel tests. Some guidelines do exist that are the result of parametric studies of the flow about various vehicle shapes, the most complete being the USAF/FDL Tailor-Mate studies (Ref. 3). These guidelines are not sufficiently complete to cover all possible configurations, and the designer must still resort to wind-tunnel tests of his particular configuration.

The data presented in this paper will not completely remedy this situation. Some data from a NASA-funded wind-tunnel test (Ref. 4) will be presented to show the effects of angle of attack and of a forward canard on the location and performance of normal shock inlets. The data are useful to extend the guidelines developed from Ref. 3 to a slightly different forebody shape, to different inlet shapes, and to the effects of a canard.

2. SUPERSONIC CRUISE AIRCRAFT

An analytical study showing the effects of angle of incidence on inlet location for a hypothetical supersonic cruise aircraft will be discussed in this section. The geometry of the hypothetical cruise aircraft will be discussed first. The analytical methods for computing the forebody flow, the inlet flow, and the method for interacting these two computations will be discussed next, followed by a presentation of the computational results and the implications for supersonic cruise aircraft design.

2.1 Hypothetical Aircraft Configuration

Rather than selecting for investigation an existing aircraft configuration, a generalized configuration was chosen that would be somewhat similar to cruise aircraft and yet be easily amenable to analysis by the existing methods. The basic fuselage has an elliptical cross section (major to minor axis ratio of 3) with a tangent-ogive planform (length to width ratio = 3.5), as shown in Fig. 1. Four different inlet locations were chosen which serve to illustrate the basic problems encountered in inlet placement.

A mixed compression axisymmetric inlet was chosen, since the internal flow code is limited to that configuration. A well known and researched M = 2.65-inlet configuration (see Ref. 5 and Fig. 2) was chosen as being typical of application to supersonic cruise aircraft. As indicated in Fig. 2, the minimum area of the inlet remains at a nearly constant $\bar{Z}$ as the centerbody is translated forward by $\Delta\bar{Z}$. Nondimensional coordinates of the inlet contours are given in Table 1. For most of this study, the axis of symmetry of the inlet was maintained parallel to the axis of symmetry of the fuselage.

TABLE 1. INLET COORDINATES

Centerbody				Cowl			
$\frac{Z}{r_c}$	$\frac{r}{r_c}$	$\frac{Z}{r_c}$	$\frac{r}{r_c}$	$\frac{Z_c}{r_c}$	$\frac{r}{r_c}$	$\frac{Z_c}{r_c}$	$\frac{r}{r_c}$
0	0	4.000	0.6460	0	1.000	1.750	0.8806
Straight taper		4.050	0.6477	Straight taper		1.800	0.8758
2.560	0.4055	4.088	0.6481	0.175	1.0046	1.833	0.8738
2.650	0.4202	4.125	0.6477	0.250	1.0062	Straight taper	
2.750	0.4367	4.175	0.6461	0.325	1.0073	2.000	0.8662
2.850	0.4540	4.225	0.6437	0.375	1.0077	2.025	0.8652
2.950	0.4721	4.300	0.6381	0.425	1.0078	2.050	0.8647
3.050	0.4907	4.400	0.6285	0.500	1.0074	2.075	0.8645
3.150	0.5103	Straight taper		0.575	1.0062	Straight line	
3.250	0.5301	4.750	0.5916	0.650	1.0042	2.175	0.8645
3.350	0.5509	4.850	0.5793	0.725	1.0011	2.275	0.8655
3.450	0.5721	4.950	0.5640	0.800	0.9972	2.475	0.8700
3.550	0.5940	5.050	0.5468	0.875	0.9921	2.675	0.8760
3.650	0.6140	5.150	0.5289	0.950	0.9862	2.875	0.8821
3.700	0.6218	5.250	0.5066	1.025	0.9792	3.075	0.8905
3.750	0.6278	5.350	0.4807	1.100	0.9712	3.175	0.9001
3.800	0.6329	5.400	0.4640	1.175	0.9622	3.375	0.9295
3.850	0.6370	5.450	0.4430	1.250	0.9520	3.575	0.9582
3.900	0.6407	Straight taper		1.350	0.9379	3.675	0.9675
3.950	0.6437	5.650	0.3600	1.450	0.9235	3.775	0.9733
		Straight line		1.550	0.9093	3.875	0.9766
		8.565	0.3600	1.650	0.8949	3.975	0.9784
				1.700	0.8875	4.165	0.9800
						Straight line	
				Engine face		4.475	0.9800

2.2 Analytical Method

The analytical method used in this paper consists of three main components: (1) a technique for computing the supersonic flow about a fuselage of arbitrary cross section at angle of attack, the Kutler code; (2) a technique for computing the supersonic flow in a mixed compression, axisymmetric inlet with nonuniform upstream flow; and (3) a method to couple these two techniques so that a combined solution can be obtained.

The two flow computation techniques have a common basis, the finite-difference, shock-capturing technique described in Ref. 1. A brief description of the general features of the shock-capturing technique and details relevant to each technique are given below.

2.3 Shock-Capturing Technique

The finite-difference, shock-capturing technique described here consists of solving the equations of motion, written in conservative form, between the body and some outer computational boundary. The equations of motion are written in the following form:

$$E_z + F_r + G_\phi + H = 0$$

The terms E, F, G, and H are vector components defined as:

$$E = \begin{bmatrix} \rho u \\ kp + \rho u^2 \\ \rho uv \\ \rho uw \end{bmatrix} \quad F = \begin{bmatrix} \rho v \\ \rho uv \\ kp + \rho v^2 \\ \rho vw \end{bmatrix} \quad G = \frac{1}{r}\begin{bmatrix} \rho w \\ \rho uw \\ \rho vw \\ kp + \rho w^2 \end{bmatrix} \quad H = \frac{1}{r}\begin{bmatrix} \rho v \\ \rho uv \\ \rho(v^2 - w^2) \\ 2\rho vw \end{bmatrix}$$

A complete set of equations is obtained by employing the energy equation in the following form:

$$p = \rho(1 - q^2)$$

where

$$q = \sqrt{u^2 + v^2 + w^2}$$

The solution of these equations throughout a supersonic flow field proceeds from a plane wherein all the flow properties are known to a subsequent downstream plane. Spacing between the planes is controlled by the minimum domain of influence, that is, signal propagation along Mach lines, of all of the points in the known plane. Spacing between the planes or step size less than the above, Courant number less than one, can be used in some cases to improve accuracy.

In the shock-capturing solutions presented in this paper, MacCormack's second-order accurate finite-difference algorithm (Ref. 1) was used to obtain the conservative variables at each point in the downstream plane. This algorithm is a two-step process using first the following predictor equation

$$\overline{E_{ij}^{n+1}} = E_{ij}^n - \frac{\Delta Z}{\Delta \xi}\left(F_{i+1,j}^n - F_{ij}^n\right) - \frac{\Delta Z}{\Delta \phi}\left(G_{i,j+1}^n - G_{ij}^n\right) - \Delta Z H_{ij}^n$$

and subsequently, the following corrector equation:

$$E_{ij}^{n+1} = \frac{1}{2}\left[E_{ij}^n + \overline{E_{ij}^{n+1}} - \frac{\Delta Z}{\Delta \xi}\left(\overline{F_{ij}^{n+1}} - \overline{F_{i-1,j}^{n+1}}\right) - \frac{\Delta Z}{\Delta \phi}\left(\overline{G_{ij}^{n+1}} - \overline{G_{i,j-1}^{n+1}}\right) - \Delta Z \overline{H_{ij}^{n+1}}\right]$$

After each step, the conservative variables must be decoded to find the physical variables at each point. Barred superscripts denote predicted values.

Further, both techniques use a common method for determining the flow along the body surface which is the inner computational boundary. After the flow is predicted at the body, the velocity vector will not necessarily satisfy the surface tangency condition. A small, local Prandtl-Meyer turning is imposed to satisfy the tangency condition, and the predicted flow variables are adjusted accordingly. A direct consequence of this approach is that the body surface becomes a constant entropy surface, even across discontinuities in surface curvature or shock wave reflections. The method does, however, give an accurate indication of surface pressures when compared to more accurate calculations, or experimental data (see Ref. 2).

The two techniques differ in their treatment of the outer boundary conditions. This difference is discussed in the following paragraphs.

2.3.1 Forebody Solutions

The outer computational boundary for the forebody code is the bow shock wave, which is maintained as a discrete shock wave in the solution. Conditions at the shock wave are found by solving the Rankine-Huguniot equations at each computational point on the shock wave. All other shock waves that are generated within the solution are captured by the numerical technique and diffused over several streamwise mesh points. Presently, the forebody code is limited to flows at angle of attack, that is, yaw or sideslip cannot be considered. For detailed information of the forebody technique, the reader should refer to Ref. 1.

2.3.2 Inlet Solutions

The outer computational boundary for the inlet code is an arbitrary conical surface that is sized to contain the conical shock from the centerbody tip. Flow properties at this computational boundary must be known, either input as uniform flow or, as will be described later, obtained from another computational technique, such as a forebody flow-field solver. In this solution, the centerbody conical shock wave and all other shock waves are captured by the numerical technique and diffused over several streamwise mesh points.

Since several modifications to the inlet code described in Ref. 2 have been made to allow solution of flows wherein the initial flow is nonuniform, some discussion of these modifications is appropriate. As shown in Fig. 3(a), the computation of the inlet flow is divided into three domains: conical flow, external flow, and internal flow.

A small region of conical flow is computed at the centerbody tip in order to obtain a starting solution. This is, of course, an approximation since conical flow does not exist for flows with nonuniform upstream conditions. However, if this region is kept sufficiently small, then the effect of this approximation should also be small. For inlet solutions, in a nonuniform flow field, as described here, the flow properties from the forebody flow field at coordinates of the centerbody tip are used for the free-stream conditions. The three-dimensional velocity vector at that point is resolved into a simple "angle of attack" for the cone flow solution. Further details of the conical flow solution are presented in Ref. 2.

Computation of the flow in the external flow domain required the majority of the modifications from the uniform case. First, in nonuniform flow an axis of symmetry does not necessarily exist. This requires that the flow completely around the inlet be calculated using an indexing scheme as shown in Fig. 3(b). Secondly, the nonuniform flow on the outer computational boundary must be input from another solution, in this case the forebody solution. At every point on the outer computational boundary, the nonuniform upstream flow is required; the method for obtaining this flow will be described later.

No changes to the computation of the internal flow, other than the provision to compute completely around the inlet, were required.

2.4 Coupling Technique

Coupling of two supersonic solutions together is the easiest class of problem for two interacting flows. Since there are no upstream propagating disturbances, no iteration is needed, and coupling is reduced to determining the upstream boundary conditions for subsequent downstream solutions.

In this case, output from the forebody code is in the form of the flow properties, p, ρ, u, v, and w at each point in the forebody cylindrical coordinate system Z_f, r_f, and ϕ_f. The output data are for variable radii between the body and the shock wave at constant azimuthal angles, ϕ_f within a plane of constant Z. A portion of the total forebody solution that was adequate to bound the entire inlet solution was saved on a permanent file within the computer. Essentially, data are saved over a radius interval equal to twice the inlet diameter at azimuthal angles that bound twice the included angle of the inlet diameter and Z planes from the most forward position of the centerbody tip to just aft of the cowl-lip station, as shown in Fig. 4.

Two different kinds of information can be obtained from the computational data stored in the pie shaped volume shown in Fig. 4. First, data can be obtained in any plane within the volume for definition of the flow properties within that plane. (If experimental data are available in the plane, direct comparison with that data can be made.) Secondly, computational data are obtained along the outer computational boundary for the inlet solution. Droop and toe-in of the inlet axis relative to the fuselage axis, or similarly the orientation of any plane, can be accounted for by proper transformation. The first step in obtaining the desired information from the forebody data file is to transform the coordinates of a known point in the inlet geometry or some known plane to the forebody coordinate representation. Forebody flow properties at those points are obtained from the data file using a three-dimensional linear interpolation scheme. Flow velocities from the forebody solution are then transformed to the coordinates system of the known plane.

All inlet solutions are obtained in a cylindrical coordinate system whose origin is the centerbody tip and whose Z axis is coincident with the centerline of the inlet. Points on the outer computational boundary are transformed to the cylindrical coordinate system of the forebody solution and flow properties at those points are obtained by the interpolation scheme described above. The velocities of the forebody solution are then transformed to the inlet coordinate system and entered into the inlet solution as known properties along the outer computational boundary (see Fig. 3).

2.5 Results and Discussion

The results presented here have been chosen to demonstrate three points: (1) the nature of the flow in the inlet at $M = 2.65$ and $\alpha = 0$ when it is isolated from the forebody; (2) the effect of placing the same inlet at four different locations in the forebody flow field with the forebody at $M = 2.65$ and $\alpha = 0$, and (3) the effect of forebody angle of attack on the inlet flow at the four different locations.

The pressure distribution for the isolated inlet at $M = 2.65$ and $\alpha = 0$ is shown in Fig. 5. These inlet contours have been designed to produce a nearly isentropic internal flow with effectively no internal shock waves. The $\bar{Z}$ coordinate is measured from the centerbody tip and has been normalized by the radius of cowl. For these calculations, a complete solution, defined as one with supersonic flow throughout the inlet, was obtained with the cowl in the design position, $\bar{Z}_a = 2.325$, which corresponds to a centerbody translation $\Delta\bar{Z} = 0$.

Complex three-dimensional flows are not easily amenable to simple graphical description. Variation of the flow into an isolated axisymmetric inlet at angle of attack can be bounded by the flow along the

windward, $\phi = 0°$, and leeward, $\phi = 180°$, meridians. Once the inlet is immersed in a nonuniform upstream flow, no such convenient axis of symmetry exists. An a priori specification of the meridians where the maximum and minimum pressure distributions will exist is not possible and, for the most part, computational results must be interpreted with the aid of computer graphics. However, for ease of presentation and for reasons to be discussed later, pressure distributions will be shown on the two meridians that nearly bound the pressure distributions in the inlet.

The pressure distributions in the inlets for locations 1, 2, and 3 (see Fig. 1) are shown in Figs. 6 through 8, respectively, for a forebody angle of attack of zero. In addition to the pressure distributions, the local mach number, effective angle of attack, and meridonal angle ϕ_T of the projection of the total velocity vector onto a plane normal to the fuselage Z axis at the centerbody tip are noted on the figures. A primary difference for all of these solutions from the isolated inlet solution (also included on the figures) is that the centerbody has been translated forward to maintain supersonic flow in the inlet at the slightly different Mach numbers and angles of attack. Results for location 1 are given at $\phi = 0°$ and 180° while results for locations 2 and 3 are given for $\phi = 90°$ and 270°. This is done to correspond to the windward and leeward meridians of the effective angle of attack. In all cases, it is noted that the internal pressures, and hence the peak attainable pressure recovery, are reduced due to translating the centerbody forward. Tilting the inlet axis by the effective angle of attack would reduce the required centerbody translation and hence result in higher pressure recovery. Results are not shown for location 4 because they are identical to those for location 1, except that they are all rotated through 180°. Note that location 1 appears to be the best position, as might be expected. Of the two side locations, the second appears to be the better at this angle of attack. However, as will be seen below when angle of attack effects are discussed, this will not be the case.

When the forebody angle of attack is increased to 8°, the forebody flow at the centerbody tip changes dramatically, as shown in Figs. 9-12. Optimum angle-of-attack shielding to produce a low effective angle of attack at the centerbody tip was obtained with the inlet in location 1, as also obtained experimentally in Ref. 3. However, the tip Mach number is low, requiring a large forward translation of the centerbody to maintain supersonic flow. This large centerbody translation could be reduced by changing the internal contours of the inlet to reflect a lower design Mach number.

At location 2, the basic forebody flow produces a large effective angle of attack of 11.3° at the centerbody tip. The rate of change of effective angle of attack with forebody angle of attack is greater than one in this location. This is due in part to the rapid expansion around the side of the body. Because mixed-compression axisymmetric inlets are not designed for such large angles of attack, some change in inlet orientation would be required for satisfactory inlet operation at this location. To obtain a complete solution, it was required to droop and toe-in the inlet axis relative to the fuselage by 8° and 4°, respectively. This reduced the effective angle of attack at the centerbody tip to 1.8°, as shown in parenthesis in Fig. 10. However, even then the large flow-property gradients upstream of the inlet required an extensive centerbody translation to obtain a complete solution. The variation in pressure distributions shown in Fig. 10 is, for this case, due to the large gradients in flow properties ahead of the inlet. Due to these large gradients, this location would probably be unsatisfactory for successful inlet operation at flight conditions wherein the forebody would be at angle of attack.

Both the effective angle of attack ($\alpha_T = 8.9°$ for no droop or toe-in) and Mach number are reduced at location 3. Here a droop of 6° and a centerbody translation of $\Delta\overline{Z} = 0.6$ allowed a complete supersonic solution to be obtained. More careful alignment of the inlet with the oncoming flow in this location could probably produce satisfactory inlet operation. Again, a slightly lower design Mach number might be helpful in producing better inlet performance.

The forebody flow at location 4 produced an inlet flow which was very close to the isolated inlet flow. Although the tip Mach number is above the design Mach number of 2.65, it reduces the required centerbody translation to account for angle-of-attack effects. Until significant flow separation effects occurred on the forebody, good inlet performance at angle of attack could probably be achieved in this location.

All of the forebody solutions were computed utilizing a mesh at 30 points in the azimuthal direction ($\phi = 0°$ to 180°) and 11 in the r direction with a Courant number of 0.9. Complete forebody solutions required about 200 sec of CDC 7600 computing time. Inlet solutions were obtained utilizing 20 points in the azimuthal direction ($\phi = 0°$ to 360°) and 21 points in the r direction and a Courant number of 1.0. Isolated inlet solutions required about 15 sec to compute and the nonuniform solutions required about 30 sec of CDC 7600 computing time.

The primary power of this analytical method, as demonstrated from results shown above, is its capability to determine required modifications to inlet design and location in order to achieve optimum performance when the inlet installed in a forebody flow field. Further, the effects of off-design airplane operation on inlet performance can be assessed and preliminary centerbody control schedules can be established. This should result in significantly improved designs as well as reduced design time and costs. Reductions in cost would result primarily from reductions in wind-tunnel testing to develop an optimum inlet configuration and location. Wind-tunnel testing could then focus on design refinements and on establishing final control schedules.

3. TRANSONIC AIRCRAFT

In contrast to the situation for supersonic flows, the capability to compute complex forebody and inlet flows at transonic speeds does not exist at present. However, a brief review of some current work to develop this methodology will be given here. Afterwards, a presentation will be given of some recent experimental results which will illustrate the difficulties of inlet location for operation of transonic aircraft at high angles of attack.

3.1 Transonic Computations

The computation of complex transonic flows is in a much more formative state than the computation of complex supersonic flows. Completely general methods, which can analyze the complex transonic flows discussed in this paper, must await the development of at least the next generation of computers (beyond the CDC STAR or the CRAY I, for example) as well as additional insight into the modeling of turbulent flows. However, some significant progress is being made toward computation of somewhat simpler transonic flows. Two efforts, currently under way on contract to Ames Research Center, are being developed to compute transonic flow about isolated forebodies of quite general cross section and into three-dimensional inlets, respectively. Coupling these two solution techniques together will provide the capability to solve airframe/inlet interaction problems of simple forebody-inlet configurations.

The forebody solution technique is a Navier-Stoke code being developed by Numerical Continuum Mechanics, Incorporated. An alternating-direction explicit algorithm is used to solve the full Navier-Stokes' equations. Computation of the flow proceeds in two different marching directions. Elliptic terms in either marching direction are evaluated from the previous calculation, or the initial approximation. Solution in any given marching direction reduces to solving for the flow in a plane which is either moving along the body or around the body at some uniform velocity. Typically, 8 to 10 points are included in the boundary layer with the viscous sublayer being resolved with the boundary-layer equations. Although a solution for a body of noncircular cross section has not been obtained to date, a solution of the flow about a tangent-ogive looks very encouraging in that vortex location has been accurately predicted. Completely converged solutions should be obtainable in three marching sweeps with satisfactory engineering solutions being obtainable in two sweeps. Ultimately, each sweep should take about 1 hr of CDC 7000 computer time.

The inlet solution technique is a time-dependent Euler code being developed by the General Dynamics Corporation. The goal of this effort is to generate a code that can analyze transonic flow into complex three-dimensional inlets. To date, most of the effort has focused on developing three-dimensional mesh generation techniques. A method, which is an extension of the Thompson 2-D mesh generation technique, Ref. 6, has been developed for generating three-dimensional meshes for any inlet configuration, and meshes have been generated for a circular transport type inlet with elliptical lips and for a horizontal ramp fighter type inlet with sharp lips. Future effort will concentrate on choosing the optimum computational algorithm (from a time and accuracy standpoint) and developing the computational code.

For engineering purposes, it is expected that these codes can be coupled in a noniterative mode for most problems at high subsonic ($M > 0.8$) and low supersonic flows ($M < 1.6$). Since both methods are finite difference techniques and will require a large number of mesh points to define the flow, large amounts of computer time will be required to obtain satisfactory solutions. Coupling the two solutions will require the development of special buffer programs in the interaction region to prevent the computational time from becoming totally unrealistic.

3.2 Experimental Results and Discussion

The limited data base for transonic aircraft design was discussed in the introduction. To extend the base of Ref. 3 for supersonic speeds to a different configuration, transonic speeds, and higher angles of attack, an effort was undertaken at Ames Research Center through a contract with Rockwell International (Ref. 4). This study investigated two different inlet shapes: (1) a kidney-shaped inlet in two fuselage locations with and without a forward canard, and (2) a rectangular inlet without a forward canard, but with several modifications to improve the high angle-of-attack performance (e.g., blunt lower lips, slats, and turning vanes).

3.2.1 Kidney-Shaped Inlets With and Without a Forward Canard

The forebody of the aircraft configuration, including the canard, is shown in Fig. 13. At the inlet face station, the inlet could be moved to two different locations: a high-shoulder location and a low-shoulder location, as shown in Fig. 14. The inlet was a kidney-shaped, normal-shock inlet having sharp lips for efficient supersonic flight. The width of the inlet face is about 1/7 of the half-span of the canard, whose deflection angle could be varied. Maximum chord of the canard was about 0.35 m.

All of the data discussed here were taken at a constant Mach number of 0.9 and a Reynolds number of 19×10^6/m. For subsonic inlet performance, it is usually customary to show pressure recovery versus mass-flow ratio at constant Mach number, model attitude, and geometry. Direct comparison of the effects of model attitude and geometry are often hard to make in this format. The data shown here will be for a mass flow ratio of 0.8 in order to remove one variable for ease of comparison. In some cases, showing inlet performance at a constant mass flow ratio will not show the total performance capability of a particular configuration, but the conclusions that will be drawn from this presentation will not be compromised by this restriction.

Total pressure recovery for the inlet in both positions, and without a forward canard, is shown in Fig. 15. As can be seen, nearly identical performance is obtained in both inlet locations up to an angle of attack of 20°. Additional tuft studies show little change in flow angularity at the two locations. Within the limitations of the geometric variations with this model, there seems to be little effect of angle of attack upon inlet location.

Pressure recovery, as a function of angle of attack for the lower and upper shoulder locations with a forward canard, is shown in Figs. 16 and 17, respectively. From Fig. 16 it is apparent that the performance at the inlet in the lower shoulder location is very sensitive to canard deflection angle. Although there seems to be some flow aligning or straightening effect of the canard, inlet performance seems to be more dependent on whether the canard wake is ingested into the inlet.

In contrast, the canard has a beneficial effect for the upper shoulder location where, as shown in Fig. 17, the pressure recovery is improved at all angles of attack for the canard deflection angles shown. Tuft studies show that straightening or aligning of the flow is effected by the canard at the upper shoulder location and there is no evidence that the canard wake is ingested into the inlet. Here, the canard is providing similar benefits to the fuselage and wing shielding obtained at supersonic speeds in Ref. 3 for the Tailor-Mate configurations. Proper integration of a forward canard and an inlet can be effective in improving the angle of attack performance of the inlet.

A limited investigation of the angle of yaw (or sideslip) effects upon inlet performance was conducted. Although no detailed data will be given here, the results will be discussed qualitatively. Data were obtained only for the inlet in the upper shoulder location with a forward canard at zero deflection. At an angle of attack of 4°, sideslip angles up to ±10° had little effect on inlet performance. At an angle of attack of 12°, some, but not drastic, loss in inlet performance was noted at a yaw angle of 10° for the windward inlet.

3.2.2 Rectangular Inlet

A rectangular inlet was mounted at the midshoulder location on the fuselage, as shown in Fig. 14, but without the forward canard shown in Fig. 13. Various lower-lip modifications were the primary geometric variables. Besides the two shown in Fig. 18, several others were tested: different slat positions, lip bluntness, and a turning vane.

Although detailed test results will not be presented, some qualitative discussion of the results is merited. The two-lip modifications shown in Fig. 18 provided the best performance, but were definitely not optimum. The internal slat configuration provided equal or better performance at high angles of attack than did the other configurations tested, including the kidney-shaped inlets. Very good high angle-of-attack performance was also provided by the thick, low-lip configuration, but this configuration was mass-flow limited at low angles of attack. Also, the blunt lip would incur a serious drag penalty at supersonic speeds. A thin lower lip with an inflatable boot might generate a blunt lip to obtain good high angle-of-attack performance and yet not have large supersonic drag.

4. CONCLUDING REMARKS

A computational method for coupling a three-dimensional supersonic forebody code and a three-dimensional supersonic inlet code together has been described. Computational results for a hypothetical supersonic configuration have been obtained. These results show the effects of angle of attack on inlet performance for four different inlet locations. The power of this computational method to indicate inlet location, orientation, and centerbody control schedule for optimum design and off-design performance is demonstrated by the computational results.

A brief description of some computational work under way to develop methods for airframe/inlet integration calculations for complex transonic flows has been given. Although much remains to be done, these techniques will ultimately provide the same capability as we now have for supersonic flows. Until then, systematic experimental studies of various configurations must be conducted to build a data base.

A recent series of experiments conducted for Ames Research Center by Rockwell International add the following results to the transonic data base:

(1) The effect of angle of attack, a forward canard, and inlet location on the performance of a kidney-shaped normal shock inlet for a hypothetical highly maneuverable transonic aircraft has been shown. Proper integration of a forward canard and an inlet has been shown to improve the angle-of-attack performance of a normal shock inlet at $M_\infty = 0.9$.

(2) The effects of lower-lip modifications and turning vanes on the performance of a rectangular normal shock inlet were investigated. Both a slat arrangement and a blunt lower lip provided very good high angle-of-attack performance at $M_\infty = 0.9$. The blunt lip produced a low mass-flow ratio at low angles of attack and would generate large supersonic drag.

REFERENCES

1. Kutler, P., Reinhardt, W. A., and Warming, R. F.: Multishocked, Three-Dimensional Supersonic Flowfields with Real Gas Effects. AIAA J., vol. 11, 5, May 1973, pp. 657-664.

2. Presley, L. L.: Comparison of a Shock-Capturing Technique with Experimental Data for Three-Dimensional Internal Flows. NASA SP-347, pt. 1, 1975, pp. 623-642.

3. Serber, Lewis E.: Effect of Forebody Shape and Shielding on 2-D Supersonic Inlet Performance. AIAA Paper 75-1183, AIAA/SDE 11th Propulsion Conf., October 1975, Anaheim, California.

4. Martin, Arnold W.: Investigation of Normal Shock Inlets for Highly Maneuverable Aircraft. NASA CR 137970.

5. Smetlzer, D. B. and Sorensen, N. E.: Tests of a Mixed Compression Axisymmetric Inlet with Large Transonic Mass Flow at Mach Numbers 0.6 to 2.65. TN D-6971, 1972, NASA.

6. Thompson, J. F., Thames, F. C., and Martin, W. C.: Automatic Numerical Generation of Body-Fitted Curvilinear Coordinate System for Field Containing Any Number of Arbitrary Two-Dimensional Bodies. J. Computation Physics, vol. 15, no. 3. July 1974, pp. 299-319.

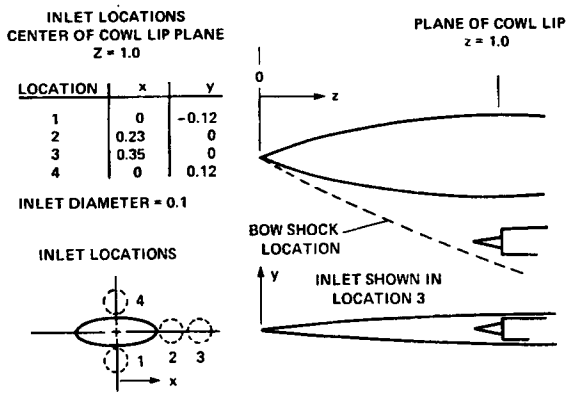

Fig. 1. Hypothetical supersonic cruise configuration.

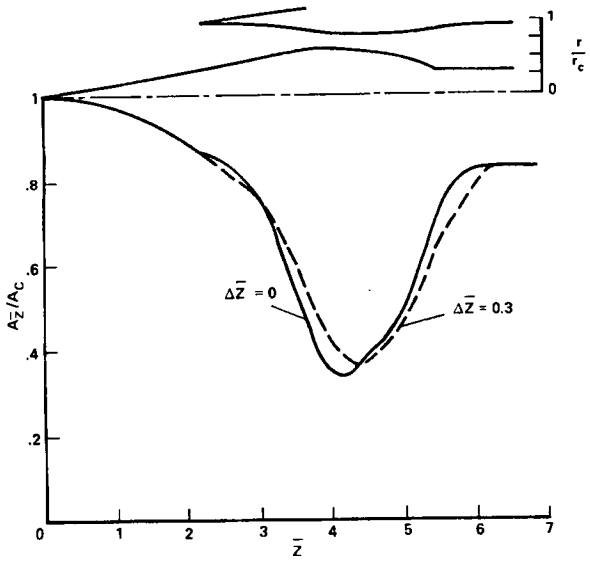

Fig. 2. Supersonic inlet contours and area distribution.

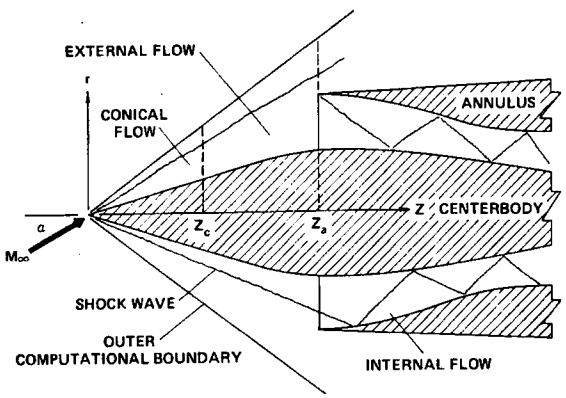

(a) Domains of inlet solution.

Fig. 3. Conceptual details of inlet solution.

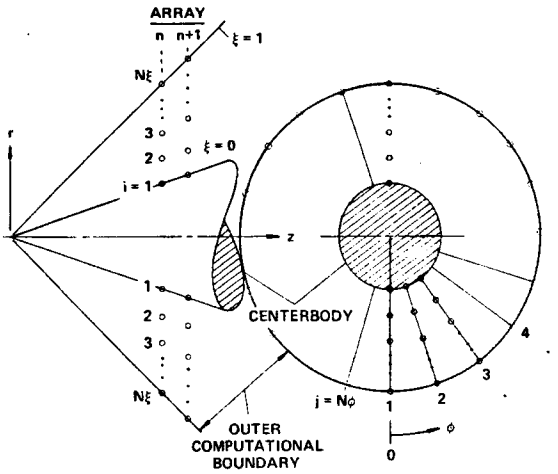

(b) Indexing scheme for inlet solutions.

Fig. 3. Concluded.

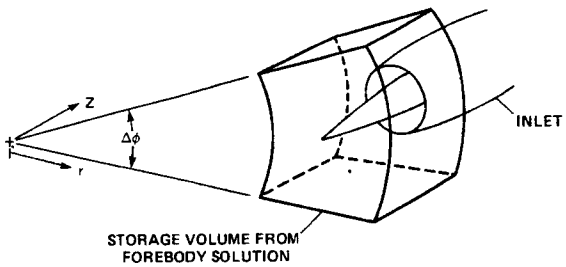

Fig. 4. Saved data volume from forebody solution.

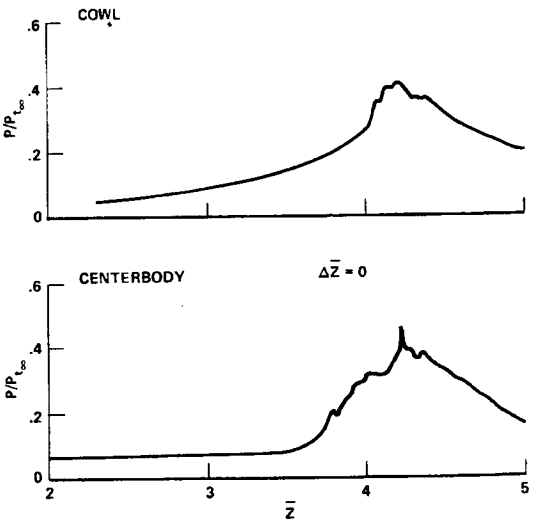

Fig. 5. Static pressure distribution, M = 2.65, α = 0, $\Delta\bar{Z}$ = 0.0.

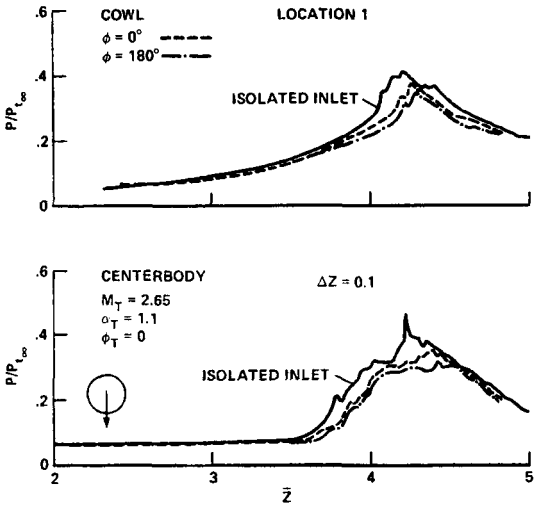

Fig. 6. Static pressure distribution, location 1 forebody: M = 2.65, α = 0.

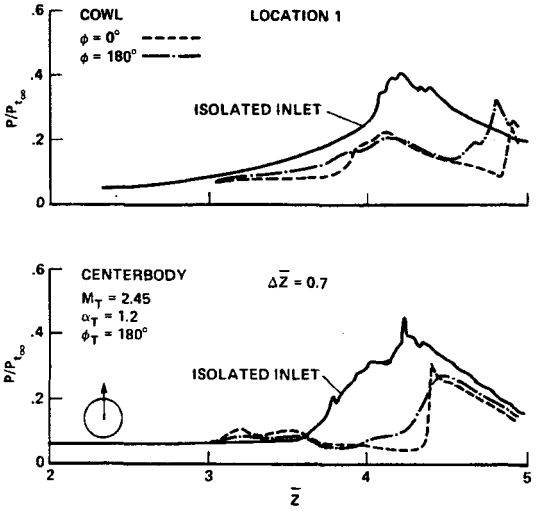

Fig. 9. Static pressure distribution, location 1 forebody: M = 2.65, α = 8°.

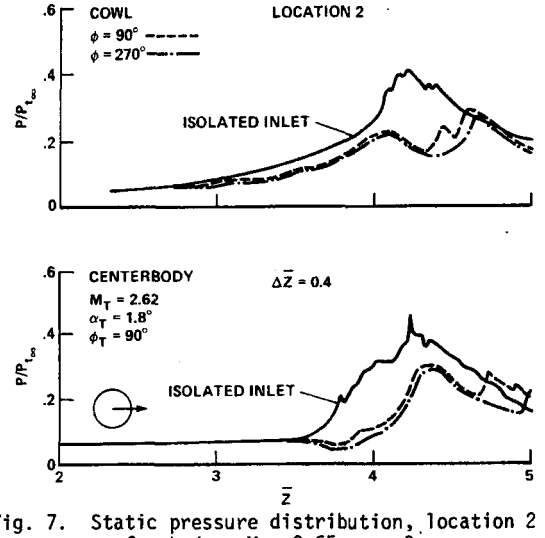

Fig. 7. Static pressure distribution, location 2 forebody: M = 2.65, α = 0.

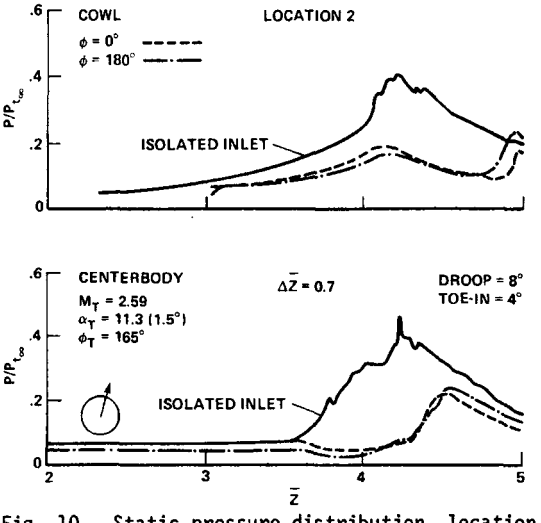

Fig. 10. Static pressure distribution, location 2 forebody: M = 2.65, α = 8°.

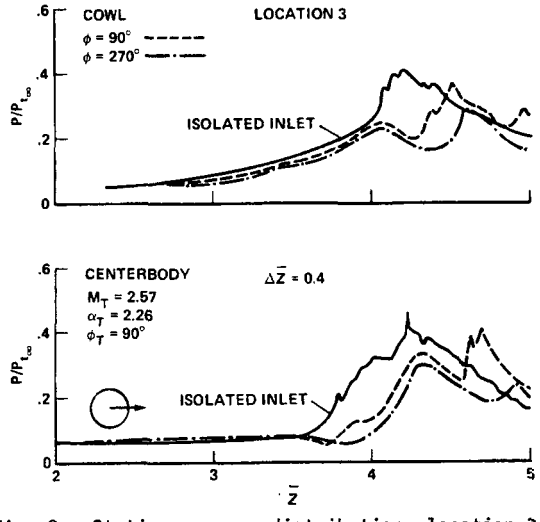

Fig. 8. Static pressure distribution, location 3 forebody: M = 2.65, α = 0.

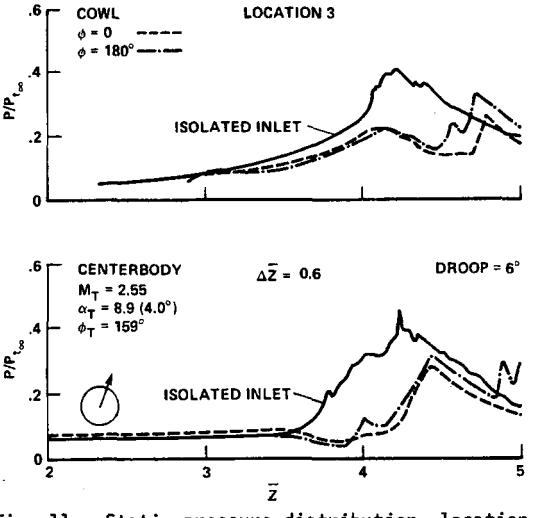

Fig. 11. Static pressure distribution, location 3 forebody: M = 2.65, α = 8°.

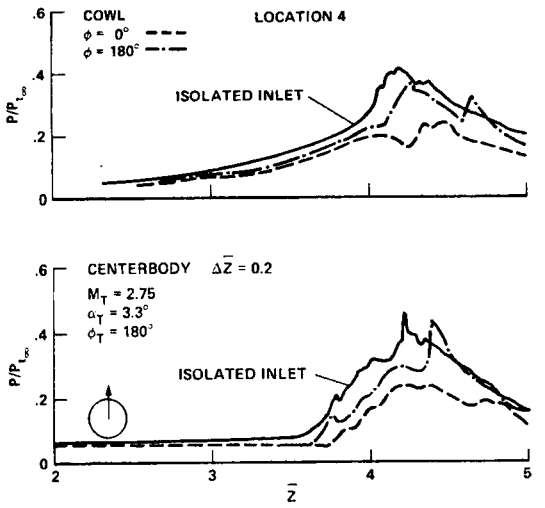

Fig. 12. Static pressure distribution, location 4 forebody: M = 2.65, α = 8°.

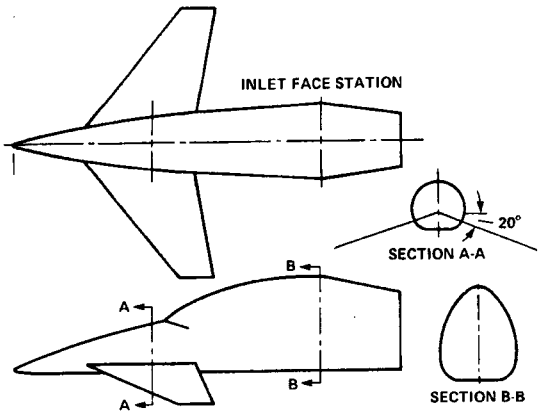

Fig. 13. Hypothetical highly-maneuverable transonic aircraft configuration.

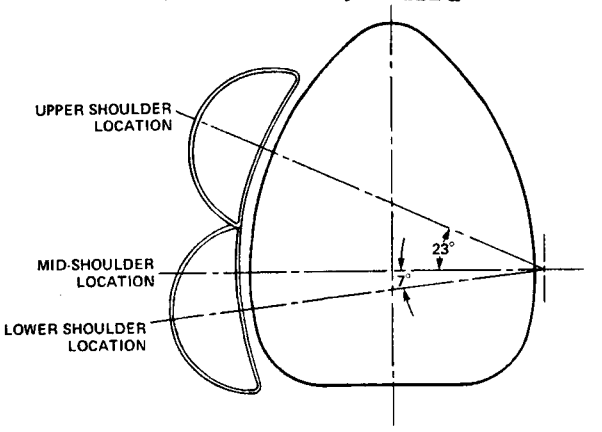

Fig. 14. Inlet shape and location.

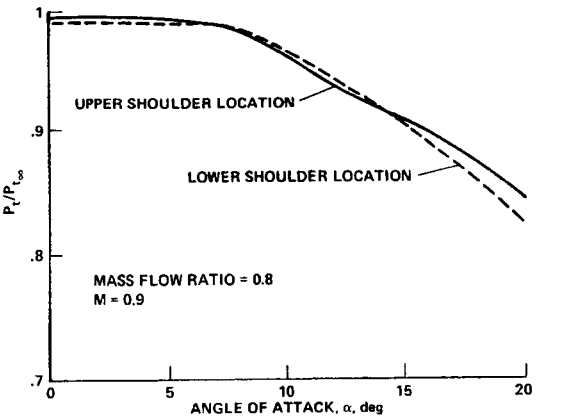

Fig. 15. Comparison of angle-of-attack performance for two inlet locations.

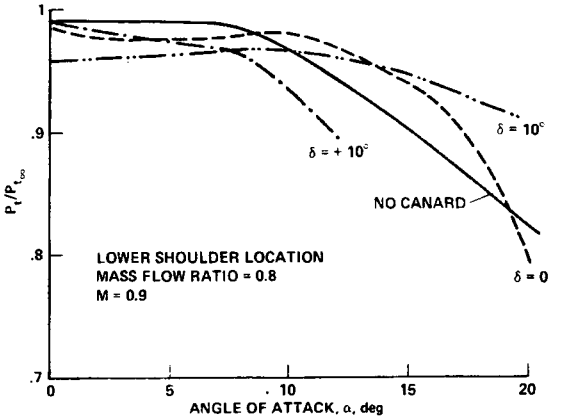

Fig. 16. Effect of canard deflection angle on low shoulder location inlet performance.

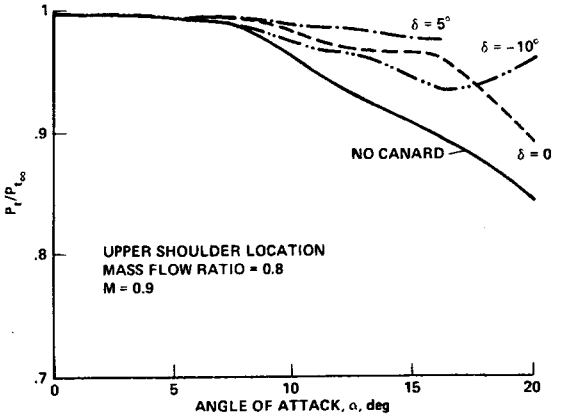

Fig. 17. Effect of canard deflection angle on upper shoulder location inlet performance.

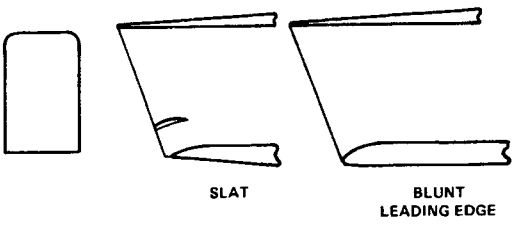

Fig. 18. Rectangular inlet lower lip modifications.

1. Report No.	2. Government Accession No.	3. Recipient's Catalog No.
NASA TM-78530		

4. Title and Subtitle	5. Report Date
HIGH ANGLE OF INCIDENCE IMPLICATIONS UPON AIR INTAKE DESIGN AND LOCATION FOR SUPERSONIC CRUISE AIRCRAFT AND HIGHLY MANEUVERABLE TRANSONIC AIRCRAFT	6. Performing Organization Code

7. Author(s)	8. Performing Organization Report No.
Leroy L. Presley	A-7634
	10. Work Unit No. 505-10-31

9. Performing Organization Name and Address	11. Contract or Grant No.
NASA Ames Research Center Moffett Field, Calif. 94035	

12. Sponsoring Agency Name and Address	13. Type of Report and Period Covered
National Aeronautics and Space Administration Washington, D.C. 20546	Technical Memorandum
	14. Sponsoring Agency Code

15. Supplementary Notes

16. Abstract

Computational results which show the effects of angle of attack on supersonic mixed-compression inlet performance at four different locations about a hypothetical forebody have been obtained. These results demonstrate the power of the computational method to predict optimum inlet location, orientation, and centerbody control schedule for design and off-design performance.

The effects of inlet location and a forward canard on the angle-of-attack performance of a normal shock inlet at transonic speeds have been studied. The data show that proper integration of inlet location and a forward canard can change the angle-of-attack performance of a normal shock inlet.

Two lower lip treatments for improving the angle-of-attack performance of rectangular inlets at transonic speeds are discussed.

17. Key Words (Suggested by Author(s))	18. Distribution Statement
High angle of attack Supersonic analysis Inlet integration Transonic data	Unlimited STAR Category - 02

19. Security Classif. (of this report)	20. Security Classif. (of this page)	21. No. of Pages	22. Price*
Unclassified	Unclassified	12	

*For sale by the National Technical Information Service, Springfield, Virginia 22161